THE PADME EXPERIMENT

P. Albicocco (AdR), F. Bossi, B. Buonomo, E. Capitolo (Tec.), C. Capoccia (Tec.), S. Ceravolo (Tec.), G. Corradi (Tec.), R. De Sangro, D. Domenici, G. Finocchiaro, L.G. Foggetta, G.S. Georgiev (Ass.), A. Ghigo, F. Giacchino (AdR), P. Gianotti (Resp.), V. Kozhuharov (Ass.), B. Liberti, G. Piperno (AdR), A. Saputi (Tec.), I. Sarra (Ass.), B. Sciascia, T. Spadaro, E. Spiriti, C. Taruggi (Dott.), E. Vilucchi

1 Introduction

One of the biggest misteries in physics today, it is that the matter seen in the universe accounts only for about 5% of the observed gravity. This has triggered the idea that enormous amounts of invisible dark matter should be present.

Among the different theoretical models that try to define what dark matter could be, there are those that postulate the existence of a "Hidden Sector" populated by new particles that do not couple with those of the Standard Model (SM). The only connection within these 2 worlds could be realized by a low-mass spin-1 particle, named A', that would possess a gauge coupling of electroweak strength to dark matter, and a much smaller coupling to the SM hypercharge [1]. This Dark Photon (DP) could be the portal connecting ordinary and dark world.

The PADME experiment aims to search for signals of such a DP studying the reaction:

$$e^+e^- \rightarrow \gamma A'$$

using the positron beam of the LNF LINAC and identifying the A' as a missing mass signal.

PADME (Positron Annihilation into Dark Matter Experiment) is an international collaboration of about 50 people that involves, in addition to LNF researchers, scientists from the INFN sections of Roma1, Roma2 and Lecce, the Sapienza and Tor Vergata Universities of Rome (IT), the Salento University (IT), the Sofia University (BG), the Cornell University (USA), and the Atomki Institute of Debrecem (H).

The apparatus, built and installed in 2018, started the data taking in October.

2 The PADME experiment

The goal of the PADME experiment is to search for DPs produced in the annihilation process of the positron beam of the LNF LINAC with a thin carbon target and then identified using a missing mass technique [2].

Figure 1 shows a scheme of the apparatus whose basic elements are:

- a high intensity and low divergence positron beam, impinging on a thin, active target, capable of monitoring the beam spot;
- a vacuum chamber to avoid spurious particle interactions;
- a magnet to deflect the beam of positrons emerging from the target, with the additional task of measuring the momentum of the interacting positrons, thus improving the rejection of the Bremsstrahlung background;

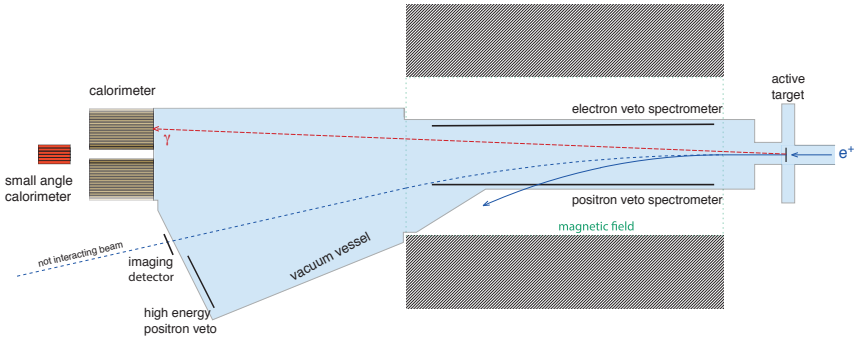

Figure 1: *The PADME experiment concept. From right to left: the active target, the positron/electron vetoes inside the magnetic field, the high energy e^+ veto near the non-interacting beam exit, the e.m. calorimeters.*

- a finely-segmented, high-resolution e.m. calorimeter, to measure the momentum of the single SM photons (ECAL).

Since the processes that mainly take place in the beam-target interaction are Bremsstrahlung and $e^+e^- \to \gamma\gamma(\gamma)$, to cut out these background events, two extra components are crucial:

- a fast Small Angle Calorimeter (SAC), placed behind the central hole of the primary one. This is used to detect and veto backgrounds photons;

- three stations of plastic scintillator slabs, located inside the vacuum chamber, two within the dipole magnet gap, and the third one on the beam exit, to veto charged particles produced in the interaction.

To have a more accurate monitoring of the beam, in the target region are installed two planes of silicon pixel detectors placed up and down stream the active diamond target. Each plane consists of two MIMOSA 28 Ultimate chips, developed for the upgrade of the STAR vertex detector [3]. These devices integrate a Monolithic Active Pixel Sensor (MAPS) with a fast binary readout. Each sensor consists of a matrix of 928×960 pixels of 20.7 μm side with a thickness of 50 μm. For the STAR experiment the chips, that dissipate 150 mW/cm^2, operate in air without cooling. For PADME, the detector has been placed in vacuum and a modified PCB has been developed by the LNF electronic service to provide cooling. In the following sections more details on the detector characterization are given.

The MIMOSA detector cannot stay on the beam line during the data taking, therefore an extra monitoring device is placed out of the vacuum on the positron beam exit trajectory. This is an array (3×2) of Timepix3 chips [4] able to record either the time-of-arrival (ToA) and the energy of the incident particles providing excellent energy and time resolutions. The silicon chip is designed in 130 nm CMOS technology and contains 256×256 pixels (55×55 μm^2). This detector has been build ad installed at LNF by the ADVACAM company [5].

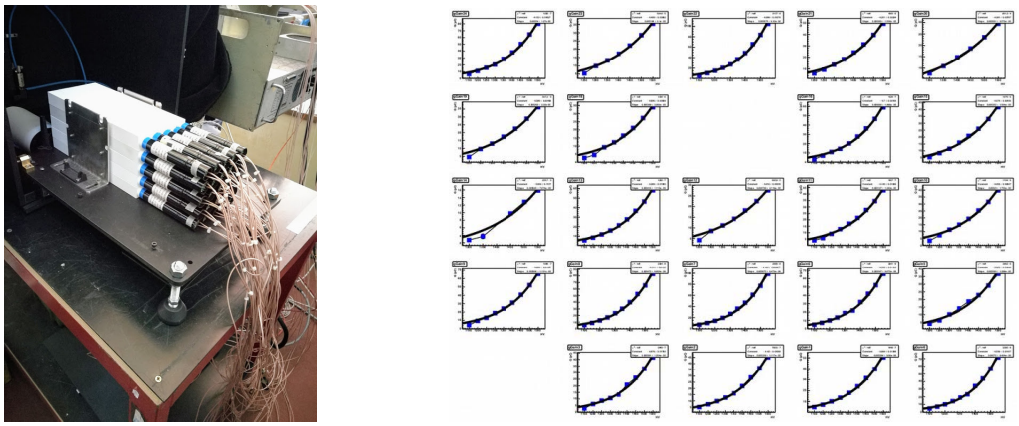

(a) (b)

Figure 2: *a) Test bench used to calibrate the scintillating units of the ECAL. b) Gain curves of different scintillating units.*

3 Activity of the PADME LNF group

During 2018 the PADME collaboration has worked to install and commission all detector components on the beam line.

In the first months of 2018, the LNF group has been involved in 3 main activities:

- test and calibration of the scintillating units constituting the main e.m. calorimeter;
- monitoring the construction of the vacuum chamber;
- preparation of the experimental hall and beam line.

To characterize and equalize the response of all scintillating units, an automatic test-stand was realized (see fig. 2a). It consisted in a light-tight box where a 5×5 matrix of crystals could be illuminated with a ^{22}Na gamma source. The source was moved in front of each unit by a step motor and the trigger signal for the measurements was produced by a small LYSO crystal detecting one of the back-to-back 511 KeV photons emitted by the ^{22}Na. By collecting data at different HVs the gain curve of each scintillating unit was determined (see fig. 2b).

The big PADME vacuum chamber ($\sim$ 1 m^3 volume) is a crucial element of the experiment that has to provide a pressure lower than 10^{-6} mbar in the whole volume downstream the interaction region. The general design of the chamber has been realized by the LNF research division mechanical service, while the construction has been committed to an external firm. It consists of 2 halves, one placed on a holding chariot standing downstream the dipole gap, while the second, tightly connected to the first, is suspended in cantilever inside the magnetic field. For this reason it has been realized using stainless steel with low magnetic permeability. Different service flanges are present on the structure to allow the passage of all needed cables and pipes. The more challenging of this flanges is the big exit circular one facing the ECAL (diam. $\sim$ 60 cm). This has to be very light in order to keep as low as possible the multiple scattering of photons, and has been realized using composite carbon-fibre material by a specialized company. Figure 3 show the side view drawing of the chamber, and a picture taken during the vacuum tests performed before the final installation.

The PADME experiment uses the positron beam accelerated to 550 MeV by the LNF LINAC. The beam line is the former BTF line 1, that since October 2018 is exclusively dedicated to the

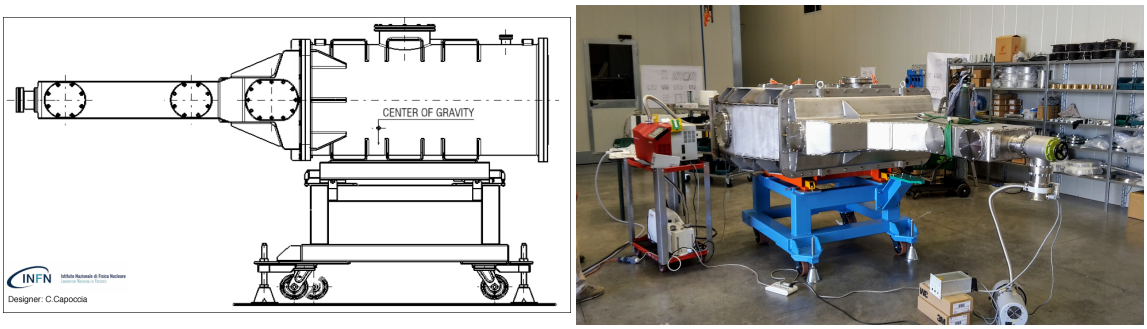

(a) (b)

Figure 3: *a) Side-view drawing of the PADME vacuum chamber. b) The chamber under test before the installation in the experimental hall.*

experiment. On a parallel line, in order to maintain the possibility to deliver beams to external users, a second line has been approved and it is under construction at LNF (BTF line 2). This is realized by splitting the LINAC beam with a new fast dipole that has been installed in June 2018 (see fig. 4). The optimization of the beam line for the needs of the PADME experiment started

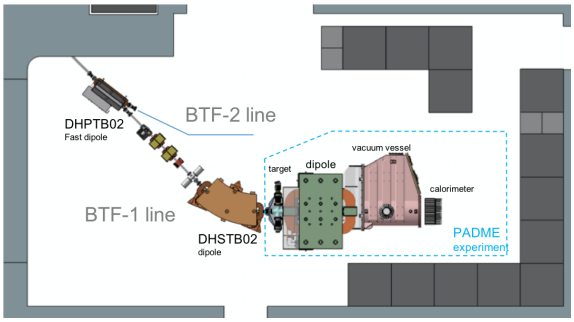

Figure 4: *Layout of the PADME beam line and arrangement of the detector in the experimental hall.*

after the summer break. The BTF staff commissioned it in September 2018 reaching the goal of $10^4 \div 10^5$ positrons/pulse with a pulse duration of about 250 ns (repetition 50 Hz). At present, these are the standard running conditions of the experiment.

In September 2018, the installation of the PADME detector components also started. Figure 5 shows pictures taken during this phase, while fig. 6 is an overview of the complete setup.

3.1 Mimosa detector characterizaton

The precise measurement of the beam parameters and the tuning of the positron beam requires the presence of a tracking device able to detect single particles. This is realized by a sequence of four MIMOSA-28 chips, to be operated in vacuum.

The chip has a limited thermal capacity due to its small thickness of only 50 μm. When operated in air the maximal temperature reaches 37 degrees Celsius, with ambient temperature of 25^o C, as seen in figure 7 left.

(a) (b) (c)

Figure 5: *a) The complete ECAL . b) The SAC during the mounting phase. c) Installation of the veto detectors inside the vacuum chamber.*

Figure 6: *The PADME experiment completely assembled in the experimental hall.*

A special mounting support was developed by the mechanical service of the research division of LNF to hold the MIMOSA carrier board in vacuum. Through a metal flange, the heat from MIMOSA is taken to a Peltier element, which is able to cool the metal frame down to 0^o C. To follow the temperature change, a 100 μA current generator connected to the MIMOSA on-chip diode is used and the required voltage between the terminals is measured. The calibration of the system was performed using a FLIR IR camera and close-to-linear response was observed in the temperature range 20^o C - 40^o C, as seen in fig. 7 right.

Before being installed in the PADME experiment the MIMOSA has been tested in a dedicated vacuum chamber. Here the pressure was slowly decreased to prevent eventual break down of the chip. The cooling proved to be efficient even at pressure below 10^{-2} bar, with MIMOSA

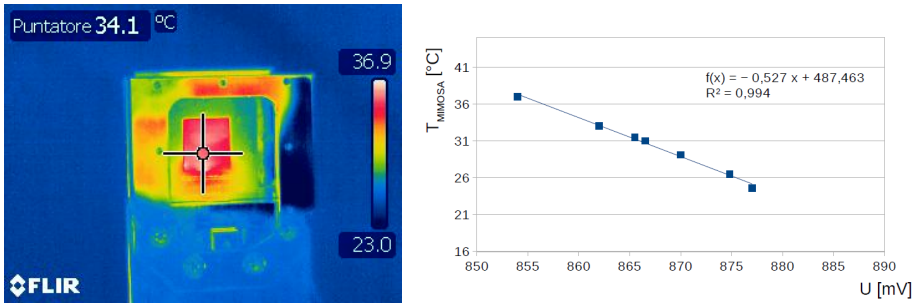

Figure 7: Temperature profile of the MIMOSA chip as measured with FLIR 335 IR camera and calibration of the on-chip diode for temperature measurement.

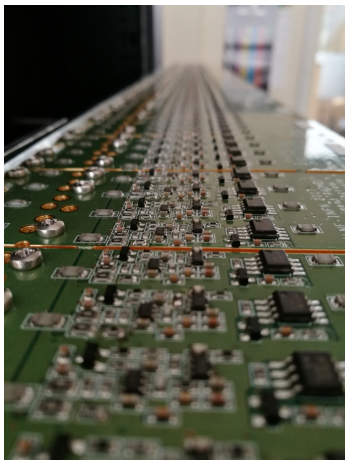

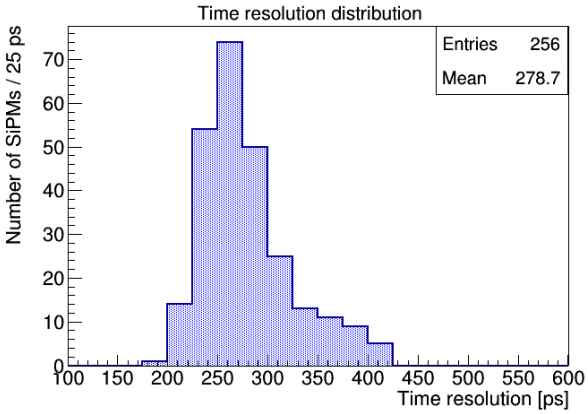

Figure 8: Front-end electronics mounted on the charged particle detectors and distribution of the measured time resolution of each SiPM channel.

temperature about 10 degrees higher than the surrounding frame.

3.2 Electronics for the charged particle detectors

Three sets of charged particle detectors are operated at PADME - the EVeto, the PVeto, and the HEPVeto. They are based on plastic scintillator bars with WLS fiber placed in a groove along the bar. The light pulse is registered by a silicon phototomultiplier. The front end electronics, shown in fig 8-left, for all of them was developed at LNF-INFN. It had to satisfy the following requirements:

- Operation in vacuum;
- Time resolution below 500 ps;
- Possibility for charge measurement.

The front end electronics consists of front end cards housing four SiPM each, providing a differential signal output, which afterwards is translated to a single ended by a controller. The controller module also sets the HV for the individual SiPMs and provides information about the current/voltage/temperature. The current consumption of the electronics per channel is 10 mA for the low voltage circuit (9 V) and 300 μA for the high voltage circuit (100 V).

The proper operation of the electronics in vacuum was checked with a custom vacuum chamber with DB50 feed-through. The temperature of the SiPM cards did not exceed 36 degrees for ambient temperature of 24 degrees and realistic passive cooling.

The time resolution was measured for each SiPM and FEE channel using a custom LED-driver and adapted mechanics. It provided short light pulses to 16 SiPMs, tested simultaneously. The time resolution of the individual SiPMs was found by a least squares minimization of the time resolutions of the time differences between couples of SiPMs. The values were studied depending on the position in the illuminated matrix due to differences in illumination. The observed performance was better than 500 ps for all the SiPMs, as seen in fig. 8. On average, the time resolution was of the order of 300 ps. All SiPM cards and controllers

4 List of Conference Talks by LNF Authors in Year 2018

Here below, it is the list of conference presentations given by LNF PADME members:

1. C. Taruggi, "Stato e Prospettive dell'esperimento", XVII edizione degli Incontri di Fisica delle Alte Energie (IFAE2018) Milano, Italy, 4-6 Apr. 2018.
2. G. Piperno, "PADME electromagnetic calorimeter", 8^{th} International Conference on Calorimetry in Particle Physics (CALOR2018), Eugene, USA, 21 - 25 May 2018.
3. P. Gianotti, "The investigation on the dark sector at the PADME experiment", 14^{th} Pisa Meeting on Advanced Detectors (PM2018), La Biodola - Isola d'Elba, Italy, 27 May - 2 Jun. 2018.
4. P. Gianotti, "The calorimeters of the PADME experiment", 14^{th} Pisa Meeting on Advanced Detectors (PM2018), La Biodola - Isola d'Elba, Italy, 27 May - 2 Jun. 2018.
5. P. Gianotti, "The investigation on the dark sector at the PADME experiment", XXXIX International Conference on High Energy Physics, Seoul, Korea, 04 - 11 Jul. 2018.
6. V. Kozhuharov, "The PADME experiment at LNF-INFN", 10^{th} Jubilee International Conference of the Balkan Physics Union, Sofia, Bulgaria, 26 - 30 August 2018.
7. G. Georgiev, "Performance of the Front-End Electronics of the PADME Charged Particle Detector System", XXVII International Scientific Conference Electronics (ET2018), Sozopol, Bulgaria, September 13 - 15, 2018.

5 Publications

Here below, it is the list of papers published by PADME LNF members in 2018:

1. P. Gianotti, "The PADME Detector", EPJ Web Conf. **170**, 01007 (2018).
2. G. Piperno, "Dark Photon Search with PADME at LNF", Int. J. Mod. Phys. Conf. Ser. **46**, 1860047 (2018).
3. G. Georgiev, V. Kozhuharov, L. Tsankov, "The PADME Tracking System", Rad. & App. Vol. **1 no. 3**, 183 (2018).
4. P. Gianotti, "Status and prospects for the PADME experiment at LNF", EPJ Web Conf. **166**, 00009 (2018).
5. C. Taruggi, "The PADME calorimeter: Performance of the prototype", Nuovo Cim. **C41** no.1-2, 92 (2018).
6. G. Piperno, "Dark photon search with the PADME experiment", Nuovo Cim. **C41** no.1-2, 50 (2018).
7. F. Ferrarotto *et al.*, "Performance of the Prototype of the Charged-Particle Veto System of the PADME Experiment", IEEE Trans. Nucl. Sci. **65** no. 8 (2018).
8. G. Georgiev *et al.*, "Performance of the Front-End Electronics of the PADME charged particle detector system", ISBN: 978-1-5386-6692-0, doi:10.1109/ET.2018.8549581

References

1. B. Holdom, Phys. Lett. B 166, 196 (1986).
   M. Pospelov, Phys. Rev. D 80, 095002 (2009).

2. M. Raggi and V. Kozhuharov, Rivista del Nuovo Cimento 38 no. 10, (2015).
   DOI 10.1393/ncr/i2015-10117-9

3. I. Valin *et al.*, JINST 7, C01102 (2012).

4. T. Poikela *et al.*, JINST 9, C05013 (2014).

5. ADVACAM s.r.o., U Pergamenky 12, 17000 Praha 7, Czech Republic, (`https://advacam.com`).